2023

A Label-Free Fiber Ring Laser Biosensor For Ultrahigh Sensitivity Detection of Salmonella Typhimurium

Shi Qiu
University of Posts and Telecommunications, Beijing, China

Bin Liu
Nanchang Hangkong University, China

Yuankui Leng
Nanchang University, China

See next page for additional authors

Funder: National Natural Science Foundation of China (Granted No. 62275015, 62175097, 62065013), Royal Society International Exchanges 2021 Round 2 (IES\R2\212135)

A label-free fiber ring laser biosensor for ultrahigh sensitivity detection of *Salmonella* Typhimurium

Shi Qiu[1,#], Bin Liu[2,#], Yuankui Leng[3], Edward Fox[4], Xian Zhou[5], Binbin Yan[1], Xinzhu Sang[1], Keping Long[5], Yanjun Fu[2], Xingdao He[2], Jinhui Yuan[1,5,*], Gerald Farrell[6], Qiang Wu[2,7,*]

1 State Key Laboratory of Information Photonics and Optical Communications, Beijing University of Posts and Telecommunications, Beijing 100876, China

2 Key Laboratory of Optoelectronic Information Science and Technology of Jiangxi Province, Nanchang Hangkong University, Nanchang 330063, China

3 State Key Lab Food Sci & Technol, Nanchang University, Nanchang, China.

4 Faculty of Health and Life Sciences, Northumbria University, Newcastle upon Tyne, NE1 8ST, United Kingdom

5 Research Center for Convergence Networks and Ubiquitous Services, University of Science & Technology Beijing, Beijing 100083, China

6 Photonics Research Centre, School of Electrical and Electronic Engineering, City Campus, Technological University Dublin, Dublin 7, Ireland

7 Faculty of Engineering and Environment, Northumbria University, Newcastle upon Tyne, NE1 8ST, United Kingdom

 # These authors have equal contributions to this paper

***** *Corresponding authors: yuanjinhui81@bupt.edu.cn; qiang.wu@northumbria.ac.uk*

Abstract The rapid detection of low concentrations of *Salmonella* Typhimurium (*S.* Typhimurium) is an essential preventive measure for food safety and prevention of foodborne illness. The study presented in this paper addresses this critical issue by proposing a single mode- tapered seven core- single mode (STSS) fiber ring laser (FRL) biosensor for *S.* Typhimurium detection. The experimental results show that the specific detection time of *S.* Typhimurium is less than 20 min and the wavelength shift can achieve -0.906 nm for an *S.* Typhimurium solution (10 cells/mL). Furthermore, at a lower concentration of 1 cell/mL applied to the biosensor, a result of -0.183 nm is observed in 9 % of samples (1/11), which indicates that the proposed FRL biosensor has the ability to detect 1 cell/mL of *S.* Typhimurium. In addition, the detection results in chicken and pickled pork samples present an average deviation of -27% and -23%, respectively, from the measured results in phosphate buffered saline. Taken together, these results show the proposed FRL biosensor may have potential applications in the fields of food safety monitoring, medical diagnostics, etc.

Keywords: Fiber ring laser biosensor, *Salmonella* Typhimurium (*S.* Typhimurium) detection, Foodborne pathogens.

1. Introduction

Outbreaks of foodborne diseases due to contamination of foods by pathogenic microorganisms causing infection present a significant burden to public health. Such outbreaks have resulted in large numbers of hospitalizations and deaths [1-3]. A particular worldwide hazard is *Salmonella enterica* serovar Typhimurium (*S.* Typhimurium) which causes infection mainly through drinking untreated water and contaminated food, resulting in serious public health problems and huge economic losses [4,5]. Although

reports suggest ingestion of more than 10^5 cells of *Salmonella* causes infection in healthy individuals, as little as 15 to 20 cells causes infection in immunocompromised or highly susceptible individuals [6,7]. However, low contamination numbers, e.g. ≤10 CFU per 100 g food, have been linked to outbreak of disease, highlighting the potential for disease even at low cell numbers, and the necessity for highly sensitive detective methods in food applications [8,9]. This highlights two important aspects of *Salmonella* contamination of food products: firstly, that foods are often contaminated at relatively low numbers; and secondly, that this may still cause cases of illness and outbreaks of salmonellosis. This necessitates highly sensitive detection methods to underpin food safety concerning this bacterial pathogen. Currently, the standard approach for detection of *Salmonella* relies on culture-based methods to recover low numbers of *Salmonella* in food and environmental samples, and subsequently detect them on selective agars. Methods such as the ISO 6579-1:2017, while having a low limit of detection (LoD), typically require at least one enrichment step, plus additional time to culture colonies on agar (in the case of ISO 6579-1:2017 for detection of *Salmonella*, this requires 3 days for presumptive positive detection, plus additional time for confirmatory tests [10]. Paradoxically, in addition to the existing traditional culture-based methods, other alternatives such as polymerase chain reaction (PCR) [11], enzyme linked immunosorbent assay (ELISA) [12,13], or loop-mediated isothermal amplification (LAMP) [14], are either time-consuming, labour-intensive, have limited sensitivity, or require complex sample pretreatment. Therefore, the development of a fast, simple and sensitive detection methods are crucial to help food safety and limit foodborne disease. In recent years, optical biosensors have been developed for such applications, due to advantages which include high sensitivity, compact form, immunity to electromagnetic interference and a capacity for multiplexed sensing [15-17]. Optical biosensors for *S.* Typhimurium detection typically rely on sensing structures such as surface plasmon resonance (SPR) [18], a fiber interferometer [19], surface-enhanced Raman scattering (SERS) [20,21] and fluorescence [22,23].

Xu *et al.* reported a Ω-shaped fiber-optic LSPR biosensor for *S.* Typhimurium detection, where the calculated LoD is 128 CFU/mL [24]. Li. *et al.* proposed an aptamer-based immuno-HCR-SERS method with a dual signal amplification capability to detect *S.* Typhimurium at an LoD of 6 CFU/mL within 3.5 h [25]. Duan *et al* developed a motor fluorescence biosensor to detect *S.* Typhimurium, where the calculated LoD of 10 CFU/mL achieved [26]. Duan *et al*. demonstrated the fluorescence and aptamer-functionalized magnetic nanoparticles-based biosensor to detect *S.* Typhimurium and *Staphylococcus aureus* (*St. aureus*) with LoDs of 5 CFU/mL and 8 CFU/mL within 40 mins, respectively [27]. Zhang *et al*. demonstrated a capillary biosensor for rapid detection of Salmonella using Fe-nanocluster amplification and smartphone imaging, achieving an LoD of 14 CFU/mL [28]. Similarly, Yi *et al*. investigated a gold nanoparticles-based colorimetric biosensor, whose theoretical LoD could achieve 16 CFU/mL [29]. Among the structures investigated, optical fiber interferometers have the advantages of a simple structure, ease of fiber coupling along with simple fabrication and readily available materials [30,31].

Typically, the spectrum of an optical fiber interferometer usually has a large wide height full width (FWHM) and a low extinction ratio (ER), which significantly limits the resolution and LoD. The integration of an erbium-doped fiber amplifier (EDFA) in the sensing system can effectively amplify the interference peak of the interference spectrum to a laser and thus obtain the narrow FWHM, high ER, and high Q factor [32]. Fiber ring laser (FRL) sensors have been proven to have important applications in measuring some physical quantities, such as humidity [33], refractive index (RI) [34], and temperature [35]. At present, there are no reports of using an FRL to realize *S.* Typhimurium sensing. It is only when

the core-to-core pitch of a seven-core fiber is small that stable energy exchange occurs between the cores and the resulting modes are called supermodes [36]. The size of the cores as well as the core-to-core pitch can have a large effect on the supermodes. Tapering a seven-core fiber can flexibly adjust the coupling strength between the cores, and further adjust the interference effect of the supermodes, and also enhance the evanescent field, so as to achieve higher sensitivity. As *S.* Typhimurium is captured by the functionalized fiber surface, this results in a change in the interference length of the supermodes, which leads to measurable spectral shifts.

In this paper, we propose a single mode- tapered seven core- single mode (STSS) FRL biosensor for *S.* Typhimurium detection. A narrow FWHM and high ER have been achieved by integrating the STSS fiber into an EDFA FRL system, as an effective means to improve sensitivity and measurement accuracy for *S.* Typhimurium. The results demonstrate that 10 cells/mL of *S.* Typhimurium solution can be consistently detected by the proposed biosensor within 20 min. In addition, 1 cell/mL of *S.* Typhimurium solution also showed a detectable signal after continuous measurements.

2. Biosensor structure and sensing system

2.1. The STSS fiber biosensor structure and theoretical analysis

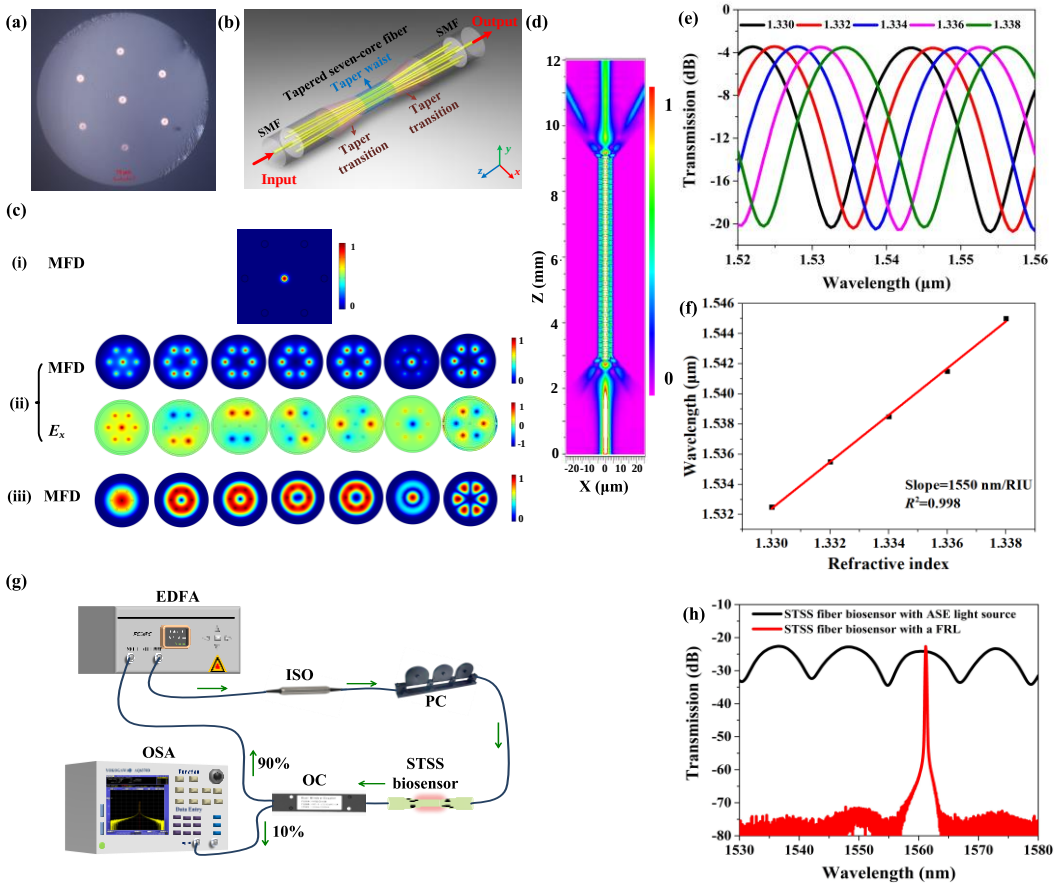

Fig. 1(a) A cross-section of the STSS fiber, (b) a three-dimensional sketch of the STSS fiber, and (c) the mode analysis at different positions of the STSS fiber, (d) the simulated transmission optical field distribution along *x*-*z* direction of the STSS fiber at wavelength 1550 nm, (e) the simulated transmission spectra and (f) the RI sensitivity in the RI range from 1.330-1.338, (g) the schematic representation of the experimental setup, and (h) the output spectra of an STSS fiber biosensor with an ASE source and with an EDFA + FRL light source.

Fig. 1(a) shows the cross-section of the untapered seven-core fiber (SCF, SM-7C1500, purchased from the FIBERCORE Company). Fig. 1(b) shows the three-dimensional diagrammatic sketch of the STSS fiber biosensor. Fig. 1(c) demonstrates the mode analysis at different positions of the tapered SCF (TSCF), focusing on the formation of supermodes supported in this fiber [36, 37], the phase relationship between different supermodes, and supermodes interference effect [38, 39]. Fig. 1(d) shows the simulated transmission optical field distribution along *x*-*z* direction of the TSCF at 1550 nm. Figs. 1(e) and 1(f) depict the simulated transmission spectra and corresponding RI sensitivity in the RI range from 1.330 to 1.338, respectively. (Supplementary Material 1.1 contains a thorough description)

2.2. The STSS FRL sensing system

Fig. 1(g) shows the schematic representation of the experimental setup in which the STSS is incorporated into a FRL arrangement containing an EDFA. Fig. 1(h) shows the comparison of output spectrum of the STSS fiber biosensor with and without an FRL. (Supplementary Material 1.2 contains a thorough description)

3. Material and methods

3.1. The RI sensitivity of the STSS FRL biosensor

The RI measurement of the proposed STSS FRL biosensor was conducted experimentally, with a RI sensitivity of 1213.024 nm/RIU, in the RI ranges of 1.3333-1.3355. (Supplementary Material 2.1 contains a thorough description)

3.2. Functionalization of the STSS FRL biosensor

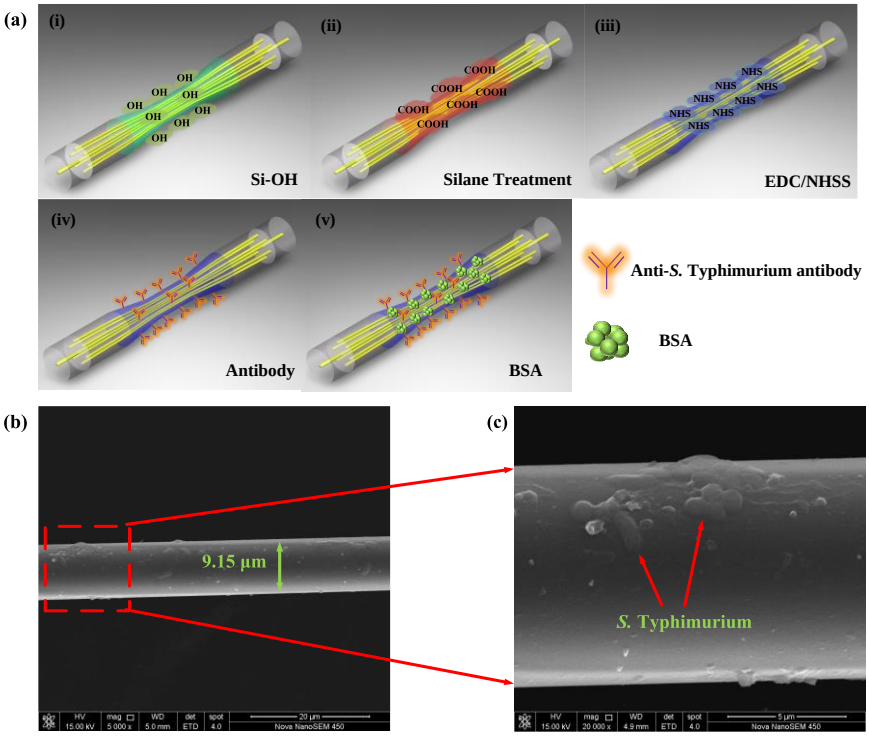

Fig. 2. (a) The modification process of the TSCF: (i) create Si-OH on the fiber surface, (ii) silane reagent treatment, (iii) EDC and NHSS solution activation, (iv) binding anti- *S.* Typhimurium antibodies, and (v) using BSA to prevent unbind sites. SEM images of (b) the waist region of the STSS fiber biosensor, and (c) a further magnified image showing *S.* Typhimurium bound to the TSCF surface.

Figs. 2(a) (i-v) show the detailed modification processes of the TSCF. Figs. 2(b)-(c) show the scanning electron microscope (SEM) images of the functionalized STSS FRL biosensor with *S.* Typhimurium bound at the waist region which has a diameter of 9.15 μm. (Supplementary Material 2.2 contains a thorough description)

4. Results and discussion

4.1. Detection of S. Typhimurium

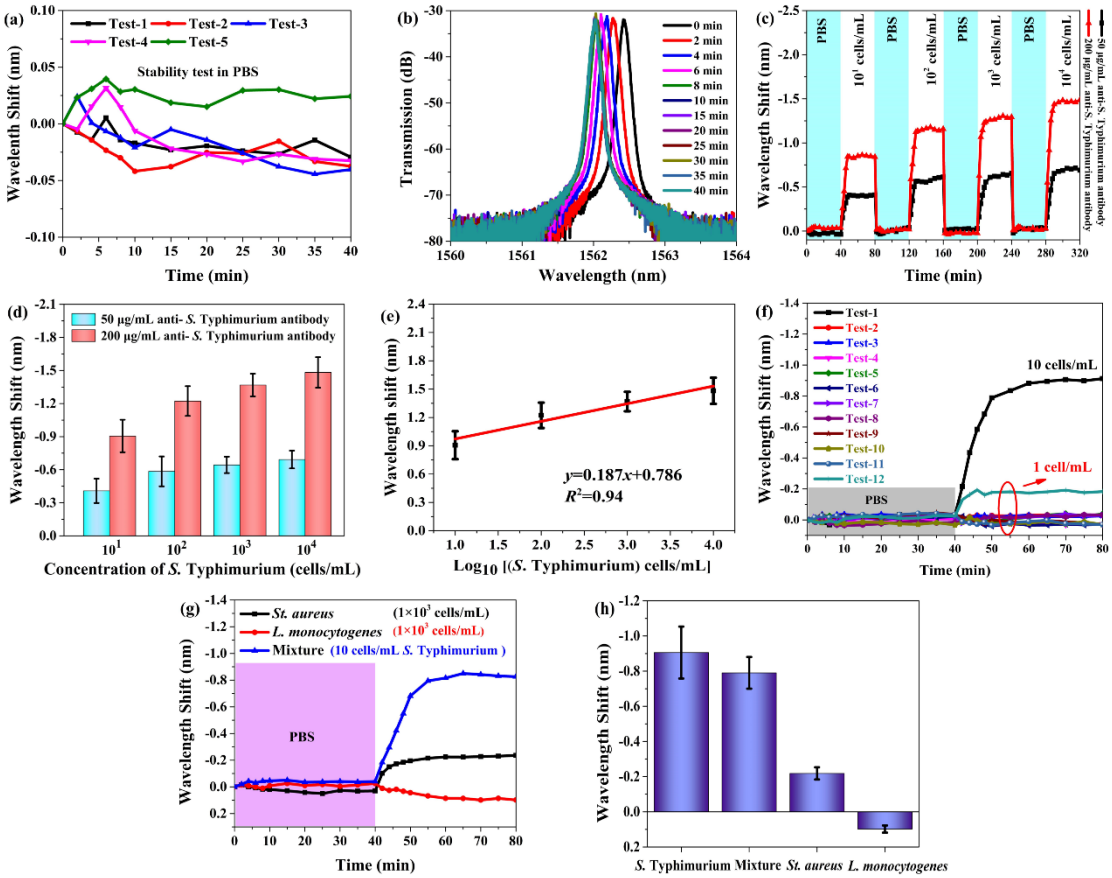

Fig. 3. (a) The stability tests of the STSS FRL biosensor, (b) the dynamic shift of spectrum of the modified STSS FRL biosensor (50 μg/mL anti- *S.* Typhimurium antibody) at a 10 cells/mL *S.* Typhimurium sample, (c) different anti- *S.* Typhimurium antibody concentrations to capture *S.* Typhimurium, (d) the reproducibility and comparison results, (e) a linear correlation between the wavelength shifts and concentrations of *S.* Typhimurium, (f) the detection processes of 1 cell/mL of *S.* Typhimurium by a STSS FRL biosensor, (g) the specificity test in *L. monocytogenes* (10^3 cells/mL), *St. aureus* (10^3 cells/mL), and mixture (this contained 10 cells/mL *S.* Typhimurium, and 10^3 cells/mL for all other species), and (h) the reproducibility results of specificity tests.

After the STSS FRL biosensors are functionalized with the *S.* Typhimurium-specific antibody and prior to undertaking *S.* Typhimurium detection, it is useful to test the spectral stability over time of the biosensors. For this five separate functionalized STSS FRL biosensors were immersed in PBS and monitored over 40 min with the results shown in Fig. 3(a). The wavelength deviations of the five sensors, all of which have the same structural parameters (the taper waist diameter is about 9 μm, the length of the taper transition regions and the taper waist are about 3 mm and 6 mm, respectively), are ±0.035 nm over 40 min, which indicates that the proposed STSS FRL biosensors have good stability over time in PBS.

After testing for spectral stability, *S.* Typhimurium was introduced. In the experiment, for the

biosensors used, the fabrication and functionalization conditions are the same, and each biosensor was used to detect S. Typhimurium at the same concentration sequentially five times, washing with PBS two times after each measurement. Each *S.* Typhimurium-containing solution applied to the biosensor is 1.1 mL. Fig. 3(b) depicts the spectra of the STSS FRL biosensor (functionalized with 50 μg/mL anti- *S.* Typhimurium antibody) when it tests a *S.* Typhimurium solution with a concentration 10 cells/mL. The wavelength shift experiences a monotonic blue-shift, whose magnitude is getting smaller as time increases. It should be noted that the *S.* Typhimurium used in this experiment were killed by heating in a water bath at 60 °C for 30 min, so the concentration unit of *S.* Typhimurium used in this work is defined as cells/mL.

Eight STSS FRL biosensors were modified with different concentrations of the anti-*S.* Typhimurium antibody, four sensors with 50 μg/mL and four sensors with 200 μg/mL. The wavelength shifts of the eight sensors were measured over time for progressively higher concentrations of *S.* Typhimurium of 10^1 cells/mL, 10^2 cells/mL, 10^3 cells/mL, and 10^4 cells/mL. PBS was also used to test the stability of the sensors between changes in concentration. It is noted that the wavelength shift is a normalized value, which is the difference between the start wavelength when immersing the fiber sensor into the analyte and the measured wavelength at different time after immersion. As seen from Fig. 3(c), the wavelength shifts increase with the increased concentration of *S.* Typhimurium for the same concentration of anti- *S.* Typhimurium antibody, which is expected as more *S.* Typhimurium is captured and attached onto the surface of the fiber biosensor. When the concentrations of *S.* Typhimurium are the same, a higher concentration of anti- *S.* Typhimurium antibody causes a larger wavelength shift, because a higher concentration of anti-*S. S.* Typhimurium antibody results in a higher capture capability and thus more *S.* Typhimurium is captured onto the fiber sensor surface.

Reproducibility is important in bio-sensing and for this reason, further tests were undertaken to determine the variation in the response of the sensors over five trials, carried out under the same conditions. Fig. 3(d) shows the reproducibility and comparison results of the biosensor functionalized with different antibody concentrations. The height of each histogram represents the average value obtained by measuring the same concentration of *S.* Typhimurium five times with a STSS FRL biosensor, and the error bars represent the corresponding deviations. From Fig. 3(d), the average peak wavelength shifts are -0.409 to -0.692 nm for the concentrations of 10^1 to 10^4 cells/mL, respectively. The concentration of anti- *S.* Typhimurium antibody has a great impact on the sensitivity. The average peak wavelength shifts are -0.906 to -1.482 nm for concentrations of anti- *S.* Typhimurium antibody of 50 to 200 μg/mL respectively. The detailed average values of the five wavelength shifts and the corresponding standard deviations are summarized in Table S1 of the Supplementary Material 3.1.

The LOD is calculated for an anti-*S.* Typhimurium antibody concentration of 200 μg/mL as this represents the most sensitive case. Fig. 3(e) depicts a linear correlation between the wavelength shifts and concentrations of *S.* Typhimurium, and the theoretical LoD of 3.63 cells/mL is obtained by the formula in Ref [21].

According to the aforementioned results, the peak wavelength shift can reach -0.906 nm in 10 cells/mL *S.* Typhimurium sample, indicating high sensitivity of *S.* Typhimurium detection, and the theoretical LoD value is 3.63 cells/mL. Therefore, to further explore the LoD of the STSS FRL biosensor, solutions with a concentration of 1 cell/mL *S.* Typhimurium were prepared. The volume of each *S.* Typhimurium solution applied to the biosensor is 1.1 mL. The detection processes of 1 cell/mL of *S.* Typhimurium by an STSS FRL biosensor are shown in Fig. 3(f). We firstly tested *S.* Typhimurium with a concentration of 10 cells/mL to prove that the fiber was successfully functionalized, after which further

tested were undertaken with *S.* Typhimurium at a concentration of 1 cell/mL with the same fiber biosensor. The wavelength shift at a concentration 10 cells/mL of *S.* Typhimurium in the first test is -0.912 nm, which is within the error range of the above test result. In the case of detection of a solution at 1 cell/mL of *S.* Typhimurium, the first 10 tests had no detectable signal response, which might be because this concentration of *S.* Typhimurium was too low and no *S.* Typhimurium cell was captured by the fiber biosensor. In the 11^{th} test of this concentration, a peak wavelength shift of -0.183 nm was observed. In summary, the above experimental results show that the proposed STSS FRL biosensor can consistently detect 10 cells/mL of *S.* Typhimurium, with 1 cell/mL of *S.* Typhimurium also showing randomly detectable signals after the continuous tests. Therefore, the LoD of the proposed STSS FRL biosensor was defined as 10 cells/mL.

4.2. Specificity test of the STSS FRL biosensor

Three sensors fabricated and functionalized with same conditions were exposed to three different types of bacterial samples: *Listeria monocytogenes* (*L. monocytogenes*), *St. aureus*, and a mixture of (*St. aureus*, *S.* Typhimurium, and *L. monocytogenes*). Each STSS FRL biosensor was used to detect one type of bacteria five times. The concentrations of both the *St. aureus* and the *L. monocytogenes* are 10^3 cells/mL, and the concentration of the *S.* Typhimurium is 10 cells/mL in the mixture samples.

Fig. 3(g) shows the peak wavelength shift in a mixture sample, *St. aureus* sample, and *L. monocytogenes* sample. From Fig. 3(g), the corresponding absolute values of the wavelength shifts are 0.826, 0.236, and 0.094 nm, respectively, which shows that the wavelength deviation in a mixture sample is much larger than that of *St. aureus* sample and *L. monocytogenes* sample. Fig. 3(h) summarizes the results and using uncertainty bars provides an insight into the reproducibility of the specificity tests. For comparison Fig. 5(h) also includes for reference the results for pure *S.* Typhimurium only. As seen from Fig. 3(h), the wavelength peak experiences a blue-shift in the pure *S.* Typhimurium, *St. aureus*, and mixture samples, while the *L. monocytogenes* samples experience a red-shift. Measurements were undertaken five times for each type of bacterial sample, and the corresponding average wavelength shifts were -0.906, -0.790, -0.219, and 0.098 nm, in *S.* Typhimurium, the mixture, *St. aureus*, and *L. monocytogenes* samples, respectively, confirming the STSS FRL biosensor's high specificity and reproducibility. The proposed STSS FRL biosensor's performance is compared with recently published results in Table 1. As seen from Table 1, an ultralow LoD of 10 cells/mL has been achieved.

Table 1. Summarized performance of the proposed STSS FRL biosensor compared with published results for *S.* Typhimurium detection

Refs	Methods	LoD	Response time
16	Surface plasmon resonance	7.4×10^4 CFU/mL	80 min
17	Fiber interferometer	247 CFU/mL	20 min
18	SERS aptasensor	4 CFU/mL	NA
19	SERS aptasensor	35 CFU/mL	1 h
20	Fluorescence	58 CFU/mL	2 h
21	Fluorescence	540 CFU/mL	NA
22	Fiber localized surface plasmon resonance	128 CFU/mL	100 min
23	SERS aptasensor	6 CFU/mL	3.5 h
24	Fluorescence	10 CFU/mL	NA

25	Fluorescence	5 CFU/mL	40 min
26	Fe-nanocluster amplification and smart phone imaging	14 CFU/mL	NA
27	Colorimetry	16 CFU/mL	NA
40	Electrochemistry	8.18 cells/mL	NA
41	Electrochemistry	500 CFU/mL	NA
42	Electrochemistry	10^3 CFU/mL	2 h
43	Electrochemistry	143 cells/mL	90 min
44	Electrochemistry	3 CFU/mL	45 min
45	Gold@platinum nanocatalyst and 3D fluidic chip optical biosensor	17 CFU/mL	1 h
This study	STSS FRL biosensor	10 cells/mL	20 min

4.3 Detection of S. Typhimurium in chicken and pickled pork samples

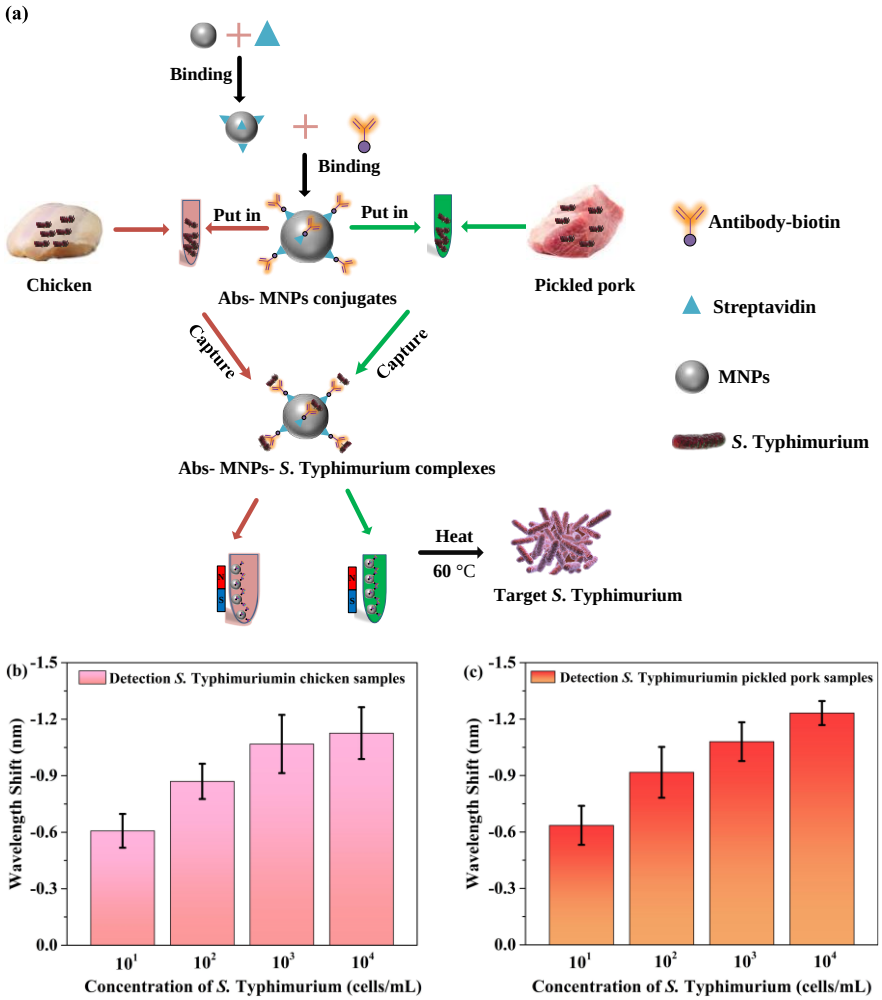

Fig. 4. (a) The schematic diagram of the IMS technology for extracting the target *S.* Typhimurium. Reproducibility tests of the 200 μg/mL anti-*S.* Typhimurium antibody functionalized STSS FRL biosensor for detection of *S.* Typhimurium: (b) in chicken samples, and (c) in pickled pork samples.

Detection of bacterial contaminants in food is essential to help ensure food safety, and is a regulated

requirement for food producers. This is typically undertaken using a series of standard, culture-based detection methodologies, which often require lengthy time periods for confirmation of results, due to the need to grow/enrich the target organisms using one or more culture media [46]. In addition, since culture-based methods can also lead to growth of non-specific targets, false negatives can be obtained due to outcompeting of the target microorganism due to growth of other species; or if the selective media cannot prevent growth of other non-specific microbial contaminants present. As such, culture-free, rapid methods present numerous advantages over traditional culture-based approaches [47]. They can improve the time to detection (e.g. from days to minutes in the case of this study), eliminate the potential false negative result due to outgrowth of competitors and/or lack of sufficient selection to prevent their growth in broth or on agar, and detect viable but not culturable (VNBC) cells. Such VNBC cells are particularly problematic to food safety and public health, as these cells are not culturable, but remain viable and can still cause infection if the contaminated food is consumed [48]; this has been demonstrated for *Salmonella* in a variety of food matrices [49]. As *S.* Typhimurium is a common foodborne pathogen and is widely found in food supply chains, and is frequently associated with poultry, livestock and other animals and associated food products, *S.* Typhimurium detection was investigated for chicken meat and pickled pork meat samples. Fig. 4(a) shows a schematic diagram of the immune-magnetic separation (IMS) technology for extracting the target *S*. Typhimurium [50]. Figs. 4(b) and 4(c) demonstrate the wavelength shifts in chicken and pickled pork samples. (Supplementary Material 3.2 contains a thorough description)

Table 2 shows the summarized results of the biosensor in different *S.* Typhimurium samples, showing the lower wavelength shift change in chicken and pickled pork samples. Overall then these results show that *S.* Typhimurium detection in real-world food samples is possible using the proposed sensor, albeit with a marginally lower sensitivity compared to PBS. This is due to the fact that the chicken and pickled pork samples have matrix interferences when compared to PBS.

Table 2. Summarized results of the proposed biosensor in different *S.* Typhimurium samples

S. Typhimurium in different sample solution	10^1 cells/mL Wavelength shift (nm)	10^2 cells/mL Wavelength shift (nm)	10^3 cells/mL Wavelength shift (nm)	10^4 cells/mL Wavelength shift (nm)
PBS	-0.906±0.15	-1.223±0.13	-1.368±0.10	-1.482±0.14
Chicken	-0.607±0.09	-0.870±0.09	-1.068±0.15	-1.126±0.14
Pickled Pork	-0.635±0.10	-0.917±0.14	-1.080±0.10	-1.232±0.06
Percentage change from PBS	-33% (Chicken) -30% (Pickled Pork)	-29% (Chicken) -25% (Pickled Pork)	-22% (Chicken) -21% (Pickled Pork)	-24% (Chicken) -17% (Pickled Pork)

5. Conclusion

In summary, an ultrahigh-sensitivity label-free STSS FRL biosensor for *S.* Typhimurium detection is proposed and experimentally investigated. By integrating the STSS fiber structure into an EDFA ring loop, very narrow FWHM and high ER of the output spectrum have been obtained. The experimental results show that the STSS FRL biosensors have good stability, high sensitivity, and fast response. When the STSS FRL biosensors are immobilized with 200 μg/mL anti- *S.* Typhimurium antibody and *S.* Typhimurium is at a concentration of 10 cells/mL in 1.1mL solution, the average wavelength shift is -0.906 nm. Furthermore, results suggest 1 cell/mL of *S.* Typhimurium can be detected by the biosensor. The STSS FRL biosensors demonstrate good specificity, showing limited cross-reactivity to other

bacterial species, including *St. aureus*, and *L. monocytogenes*; similarly, *S.* Typhimurium can be reliable detected at low concentrations in the presence of these species in a mixed species contaminated sample. Finally, *S.* Typhimurium was also detected in chicken and pickled pork samples. Compared with the results in PBS, the average percentage changes of wavelength shifts in chicken and pickled pork samples were -27% and -23%, respectively. This supports promising applications of this STSS FRL biosensor in a range of sectors, including food testing, and biomedicine.

Acknowledgements

This work is supported by National Natural Science Foundation of China (Granted No. 62275015, 62175097, 62065013), Royal Society International Exchanges 2021 Round 2 (IES\R2\212135).

References

[1] D. G. Newell, M. Koopmans, L. Verhoef, E, et al. Food-borne diseases-The challenges of 20 years ago still persist while new ones continue to emerge, *Int J Food Microbiol.*, 2010,139, S3-S15.

[2] M. Mangal, S. Bansal, S. K. Sharma, R. K. Gupta, Molecular Detection of Foodborne Pathogens: A Rapid and Accurate Answer to Food Safety, *Crit. Rev. Food Sci. Nutr.*, 2016, 56(9), 1568-1584.

[3] S. Li, Y. He, D. A. Mann and X. Deng, Global spread of Salmonella Enteritidis via centralized sourcing and international trade of poultry breeding stocks, *Nat. Commun.*, 2021, 12, 5109.

[4] J.E. Galán, Salmonella Typhimurium and inflammation: a pathogen-centric affair, *Nat. Rev. Microbiol.*, 2021, 19, 716–725.

[5] S.E. Majowicz, J. Musto, E. Scallan, F.J. Angulo, M. Kirk, S.J. O'Brien, T.F. Jones, A. Fazil and R.M. Hoekstra, The global burden of nontyphoidal Salmonella gastroenteritis, *Clin. Infect. Dis.*, 2010, 50, 2-889.

[6] M.H. Kothary and U.S. Babu, Infective dose of foodborne pathogens in volunteers: a review, *J. Food Safety*, 2010, 21, 49-68.

[7] C. Techathuvanan and D.H. D'Souza, Reverse-transcriptase loop-mediated isothermal amplification as a rapid screening monitoring tool for Salmonella enterica detection in liquid whole eggs, *J. Food Sci.*, 2012, 77, M200-M205.

[8] G. Kapperud, S. Gustavsen, I. Hellesnes, A.H Hansen, J. Lassen, J. Hirn, M. Jahkola, M.A Montenegro, R. Helmuth, Outbreak of Salmonella Typhimurium infection traced to contaminated chocolate and caused by a strain lacking the 60-megadalton virulence plasmid, *J. Clin. Microbiol*. ,1990, 28(12):2597-2601.

[9] A. Catford, K. Ganz, S. Tamber, Enumerative Analysis of Salmonella in Outbreak-Associated Breaded and Frozen Comminuted Raw Chicken Products. *J. Food Prot*.,2017, 80(5):814-818.

[10] Microbiology of the food chain - Horizontal method for the detection, enumeration and serotyping of Salmonella- Part 1: Detection of Salmonella spp. (ISO 6579-1:2017). UNE-EN ISO 6579-1-2017.2017.

[11] X. Bian, F. Jing, G. Li, X. Fan, C. Jia, H. Zhou, Q. Jin, J. Zhao, A microfluidic droplet digital PCR for simultaneous detection of pathogenic Escherichia coli O157 and Listeria monocytogenes. *Biosens. Bioelectron.*, 2015, 74, 770–777.

[12] B. Pang, C. Zhao, L. Li et al. Development of a low-cost paper-based ELISA method for rapid Escherichia coli O157:H7 detection, *Anal. Biochem.*, 2017, 542, 58–62.

[13] L. Zhu, J. He, X. Cao, K. Huang, Y. Luo, and W. Xu, Development of a doubleantibody sandwich ELISA for rapid detection of Bacillus Cereus in food, *Sci. Rep.*, 2016, 6, 16092.

[14] P.P. Kumar, R.K. Agarwal, P. Thomas, B. Sailo. et al. Rapid detection of Salmonella enterica subspecies enterica serovar typhimurium by loop mediated isothermal amplification (LAMP) test from field chicken meat samples, *Food Biotechnol*., 2014, 28, 50-62.

[15] S. Kumar, R. Singh. Recent optical sensing technologies for the detection of various biomolecules: Review, *Opt. Laser Technol*, 2021, 134:106620.

[16] N. Agrawal, B. Zhang, et al. Development of Dopamine Sensor Using Silver Nanoparticles and PEG-Functionalized Tapered Optical Fiber Structure. *IEEE T Bio-Med Eng*, 2019,67(6), 1542-1547.

[17] S. Kumar, Z. Guo, et al. MoS2 Functionalized Multicore Fiber Probes for Selective Detection of Shigella Bacteria Based on Localized Plasmon. *J. Lightwave Technol*, 2021,39(12), 4069-4081.

[18] H. Vaisocherová-Lísalová, I. Víšová, M. L. Ermini, et al. Low-fouling surface plasmon resonance biosensor for multi-step detection of foodborne bacterial pathogens in complex food samples, *Biosens. Bioelectron.*, 2016, 80(15), 84-90.

[19] S. Kaushik, A. Pandey, U. K. Tiwari and R. K. Sinha, A label-free fiber optic biosensor for Salmonella Typhimurium detection, *Opt. Fiber Techn.*, 2018, 46, 95-103.

[20] X. Ma, X. Xu, X. Yu and Z.P. Wang, SERS Aptasensor for Salmonella typhimurium Detection based on Spiny Gold Nanoparticles, *Food Control*, 2017, 84, 232-237.

[21] X. Xu, X. Ma, H. Wang and Z. Wang, Aptamer based SERS detection of Salmonella typhimurium using DNA-assembled gold nanodimers, *Microchimica Acta*, 2018, 185(7), 1-8.

[22] S. Wang, L. Zheng, G. Cai, N. Liu, M. Liao, Y. Li, X. Zhang and J. Lin, A microfluidic biosensor for online and sensitive detection of Salmonella typhimurium using fluorescence labeling and smartphone video processing, *Biosens. Bioelectron*., 2019, 140, 111333.

[23] P. L. Guo, M. Tang, S. L. Hong, X. Yu, D. W. Pang, Z. L. Zhang, Combination of dynamic magnetophoretic separation and stationary magnetic trap for highly sensitive and selective detection of Salmonella typhimurium in complex matrix, *Biosens. Bioelectron.*, 2015, 74, 628-636.

[24] Y. Xu, Z. Luo, J. Chen, Z. Huang, X. Wang, H. An and Y. Duan, Ω-Shaped Fiber-Optic Probe-Based Localized Surface Plasmon Resonance Biosensor for Real-Time Detection of Salmonella Typhimurium, *Anal. Chem.*, 2018, 90(22), 13640–13646.

[25] A. Li, P. Zuo, B.C. Ye. An aptamer biosensor based dual signal amplification system for the detection of salmonella typhimurium, *Anal. Biochem.*, 2020, 615, 114050.

[26] N. Duan, W. Sun, S. Wu, L. Liu, X. Hun and Z. Wang, Aptamer-based F0F1-ATPase biosensor for Salmonella typhimurium detection, *Sens. Actuators B Chem.*, 2018, 255(3), 2582-2588.

[27] N. Duan, S. Wu, C. Zhu, X. Ma, Z. Wang, Y. Yu and Y. Jiang, Dual-color upconversion fluorescence and aptamer-functionalized magnetic nanoparticles-based bioassay for the simultaneous detection of Salmonella Typhimurium and Staphylococcus aureus, *Anal. Chim. Acta*, 2012, 723, 1-6.

[28] H. Zhang, L. Xue, F. Huang, S. Wang, L. Wang, N. Liu, J. Lin. A capillary biosensor for rapid detection of Salmonella using Fe-nanocluster amplification and smart phone imaging, *Biosens. Bioelectron.*, 2019, 127, 142-149.

[29] J. Yi, P. Wu, G. Li, W. Xiao, L. Li, Y. He, Y. He, P. Ding, C. Chen. A composite prepared from carboxymethyl chitosan and aptamer-modified gold nanoparticles for the colorimetric determination of Salmonella typhimurium. *Microchimica Acta*, 2019, 186(11), 711.

[30] Q. Wu, Y. Qu, J. Liu, J. Yuan, S. Wan, T. Wu, X. He, B. Liu, D. Liu, Y. Ma, Y. Semenova, P. Wang, X. Xin, G. Farrell, Singlemode-Multimode-Singlemode Fiber Structures for Sensing Applications

– A Review, *IEEE Sens. J.,* 2021, 21, 12734-12751.

[31] H. Li, Y. Leng *et al.*, Tapered Microfiber MZI Biosensor for Highly Sensitive Detection of Staphylococcus Aureus, *IEEE Sens. J,* 2022, 22(6), 5531-5539.

[32] P. Niu, J. Jiang, S. Wang, K. Liu, Z. Ma, Y. Zhang, W. Chen, T. Liu, Optical Fiber Laser Refractometer Based on an Open Microcavity Mach-Zehnder Interferometer with an Ultra-Low Detection Limit. *Opt. Express,* 2020, 28(21), 30570-30585.

[33] J. Shi, D Xu, W. Xu, *et al.*, Humidity Sensor Based on Fabry–Perot Interferometer and Intracavity Sensing of Fiber Laser. *J. Lightwave Technol.*, 2017, 35(21):4789-4795.

[34] W. Bo, B. Liu, J. Liu, X. -D. He, J. Yuan, Q. Wu, Fiber Ring Laser Based on Side-Polished Fiber MZI for Enhancing Refractive Index and Torsion Measurement, *IEEE Sens. J*, 2022, 22(8), 7779-7784.

[35] J. Shi, F. Yang, W. Xu, *et al*., High-Resolution Temperature Sensor Based on Intracavity Sensing of Fiber Ring Laser, *J. Lightwave Technol.*, 2020, 38(7), 2010-2014.

[36] C. Xia, N. Bai, I. Ozdur, X. Zhou, G. Li, Supermodes for optical transmission, *Opt. Express,* 2011, 19, 16653-16664.

[37] C. Xia *et al*., Supermodes in Coupled Multi-Core Waveguide Structures, *IEEE J Set Top Quant*, 2016, 22(2), 196-207.

[38] Jose A. Flores-Bravo, R. Fernández, E. A. Lopez, J. Zubia, A. Schülzgen, R. Amezcua Correa, and J. Villatoro, Simultaneous Sensing of Refractive Index and Temperature With Supermode Interference, *J. Lightwave Technol.*,2021, 39, 7351-7357.

[39] Z. Wang, L. Zhang, Z. Ma, Z. Chen, T. Wang, F. Pang, High-Sensitivity Bending Sensor Based on Supermode Interference in Coupled Four-Core Sapphire-Derived Fiber, *J. Lightwave Technol.*, 2021, 39, 3932-3940.

[40] K. Z. Brainina, A. N. Kozitsina, Y. A. Glazyrina, Hybrid Electrochemical/Magnetic Assay for Salmonella Typhimurium Detection, *IEEE Sens. J.*, 2010, 10(11), 1699-1704.

[41] J. Dong, Z. Han, M. Xu, *et al*. A label-free electrochemical impedance immunosensor based on AuNPs/PAMAM-MWCNT-Chi nanocomposite modified glassy carbon electrode for detection of Salmonella typhimurium in milk, *Food Chem.*, 2013, 141(3), 1980-1986.

[42] X. Meng, R. Wang, Y. Li, Rapid detection of Escherichia coli O157:H7 and Salmonella Typhimurium in foods using an electrochemical immunosensor based on screen-printed interdigitated microelectrode and immunomagnetic separation, *Talanta*, 2016, 148(8), 200-208.

[43] A. S. Afonso, B. Pérez-López, R. C. Faria, *et al.*, Electrochemical detection of Salmonella using gold nanoparticles, *Biosens. Bioelectron*., 2013, 40(1), 121-126.

[44] E. Sheikhzadeh, M. Chamsaz, A. Turner, *et al.*, Label-free impedimetric biosensor for Salmonella Typhimurium detection based on poly [pyrrole-co-3-carboxyl-pyrrole] copolymer supported aptamer, *Biosens. Bioelectron*., 2016, 80, 194-200.

[45] L. Zheng, G. Cai, W. Qi, S. Wang, M. Wang, J. Lin, Optical Biosensor for Rapid Detection of Salmonella typhimurium Based on Porous Gold@Platinum Nanocatalysts and a 3D Fluidic Chip, *ACS Sens*, 2020, 5(1), 65–72.

[46] G. López-Campos, J.V Martínez-Suárez, M. Aguado-Urda, *et al*., Detection, Identification, and Analysis of Foodborne Pathogens. In: Microarray Detection and Characterization of Bacterial Foodborne Pathogens. Springer Briefs in Food, Health, and Nutrition. Springer, Boston, MA.

[47] J. Gray, Y. Hu, A. Wilson, et al., 1.07 - The Role of Genomics in Food Quality and Safety Management: Possibilities and Limitations, *Comprehensive Foodomics*, 1st Edition. 2021, 127-137.

Published by Elsevier.

[48] M. Fakruddin, K.S Mannan, S. Andrews. Viable but nonculturable bacteria: food safety and public health perspective. *ISRN Microbiology*, 2013, 703813,1-6.

[49] V. Jayeola, J.M Farber, S. Kathariou, Induction of the Viable-but-Nonculturable State in Salmonella Contaminating Dried Fruit. *Appl Environ Microbiol*, 2022, 88(2):e01733-21.

[50] S. Shan, Z. Zhong, W Lai, Y. Xiong, X.Cui, D. Liu, Immunomagnetic nanobeads based on a streptavidin-biotin system for the highly efficient and specific separation of *Listeria monocytogenes*, *Food Control*, 45 (2014),138-142.